Glycosylation, Hypogammaglobulinemia, and Resistance to Viral Infections

Dr. Mohammed A. Sadat, M.D., Ph.D.[#], **Dr. Susan Moir, Ph.D.**[#], **Tae-Wook Chun, Ph.D.**, **Paolo Lusso, M.D., Ph.D.**, **Gerardo Kaplan, Ph.D.**, **Lynne Wolfe, N.P.**, **Matthew J. Memoli, M.D.**, **Miao He, Ph.D.**, **Hugo Vega, M.D., Ph.D.**, **Leo J.Y. Kim, B.A.**, **Yan Huang, Ph.D.**, **Nadia Hussein, B.E.**, **Elma Nievas, M.D.**, **Raquel Mitchell, Ph.D.**, **Mary Garofalo, R.N.**, **Aaron Louie, B.Sc.**, **Derek C. Ireland, Ph.D.**, **Claire Grunes**, **Raffaello Cimbro, Ph.D.**, **Vyomesh Patel, Ph.D.**, **Genevieve Holzapfel, Ph.D.**, **Daniel Salahuddin, B.Sc.**, **Tyler Bristol, M.S.**, **David Adams, M.D.**, **Beatriz E. Marciano, M.D.**, **Madhuri Hegde, M.D.**, **Yuxing Li, Ph.D.**, **Katherine R. Calvo, M.D., Ph.D.**, **Jennifer Stoddard, B.S.**, **J. Shawn Justement, M.S.**, **Jerome Jacques, M.S.**, **Debra A. Long Priel, M.S.**, **Danielle Murray, M.A.**, **Peter Sun, Ph.D.**, **Douglas B. Kuhns, Ph.D.**, **Cornelius F. Boerkoel, M.D., Ph.D.**, **John A. Chiorini, Ph.D.**, **Giovanni Di Pasquale, Ph.D.**, **Daniela Verthelyi, M.D., Ph.D.**, and **Sergio D. Rosenzweig, M.D., Ph.D.**

Infectious Diseases Susceptibility Unit, Laboratory of Host Defenses (M.A.S., N.H., E.N., R.M., M.G., S.D.R.), Laboratory of Immunoregulation (S.M., T.-W.C., P.L., L.J.Y.K., A.L., R.C., J.S.J., D.M.), Laboratory of Infectious Diseases (M.J.M., T.B.), Laboratory of Clinical Infectious Diseases (B.E.M.), Laboratory of Immunogenetics (G.H., D.S., P.S.), and Primary Immunodeficiency Clinic (S.D.R.), National Institute of Allergy and Infectious Diseases, the Undiagnosed Diseases Program, National Human Research Genome Institute (L.W., H.V., Y.H. D.A., C.F.B.), the Department of Laboratory Medicine, Clinical Center (K.R.C., J.S.), and Oral and Pharyngeal Cancer Branch (V.P.) and Adeno-Associated Virus Biology Section (J.A.C., G.D.P.), National Institute of Dental and Craniofacial Research — all at the National Institutes of Health, Bethesda, the Center for Biologics Evaluation and Research (G.K., J.J.) and the Center for Drug Evaluation and Research (D.C.I., C.G., D.V.), Food and Drug Administration Clinical Services Program, Silver Spring, and SAIC-Frederick, Frederick National Laboratory for Cancer Research, Frederick (D.A.L.P., D.B.K.) — all in Maryland; the Department of Human Genetics, Emory University School of Medicine, Atlanta (M. He, M. Hegde); and the IAVI (International AIDS Vaccine Initiative) Center for Neutralizing Antibodies at TSRI and the Department of Immunology and Microbial Science, Scripps Research Institute, La Jolla, CA (Y.L.)

[#] These authors contributed equally to this work.

Summary

Genetic defects in *MOGS*, the gene encoding mannosyl-oligosaccharide glucosidase (the first enzyme in the processing pathway of N-linked oligosaccharide), cause the rare congenital disorder of glycosylation type IIb (CDG-IIb), also known as MOGS-CDG. MOGS is expressed in the

Address reprint requests to Dr. Rosenzweig at Immunology Service, DLM, CC, 10 Center Dr., Bldg. 10 2C410F, Bethesda, MD 20892, or at srosenzweig@cc.nih.gov..

endoplasmic reticulum and is involved in the trimming of N-glycans. We evaluated two siblings with CDG-IIb who presented with multiple neurologic complications and a paradoxical immunologic phenotype characterized by severe hypogammaglobulinemia but limited clinical evidence of an infectious diathesis. A shortened immunoglobulin half-life was determined to be the mechanism underlying the hypogammaglobulinemia. Impaired viral replication and cellular entry may explain a decreased susceptibility to infections.

Most proteins, including immunoglobulins, human virus receptors, and viral-coded proteins, are post-translationally modified with sugars or sugar chains that are generically referred to as glycans. Glycans are primarily classified as N-linked or O-linked oligosaccharides, depending on whether they are bound to the amide group of asparagine (N-linked) or the hydroxyl group of serine or threonine (O-linked). Glycans are associated with protein conformation, folding, solubility, stability, half-life, and antigenicity and are the moieties recognized by glycanbinding proteins. The congenital disorders of glycosylation (CDGs) are genetic disorders affecting the N-glycosylation process. CDGs are divided into defects in the synthesis of N-glycans (CDG-I) and defects in the processing of N-glycans (CDG-II). CDG-IIb (Online Mendelian Inheritance in Man database number, 606056) is caused by mutations in the gene encoding MOGS (also known as glucosidase 1). MOGS is an enzyme that is expressed in the endoplasmic reticulum and is involved in the trimming of N-glycans.[1] A single case of CDG-IIb has been reported; the patient died at the age of 74 days from severe neurologic complications.[2] In this study, we evaluated the immune system and susceptibility to viral diseases in two siblings with CDG-IIb who presented with severe hypogammaglobulinemia but not many infections.

METHODS

CASE REPORTS

Patient 1 (an 11-year-old boy) and Patient 2 (a 6-year-old girl) are the first and third children, respectively, born to a young, healthy, nonconsanguineous couple. Early in life, they each had a complex disorder characterized by dysmorphic facial features, generalized hypotonia, seizures, global developmental delay, cerebral atrophy, a small corpus callosum, optic-nerve atrophy, sensorineural hearing loss, hypoplastic genitalia, chronic constipation, and recurrent bone fractures; severe hypogammaglobulinemia was also diagnosed. The patients were evaluated for the frequency of febrile episodes, confirmed or suspected infections, receipt of antibiotics or intravenous immune globulin, and complications associated with infectious diseases and live viral vaccines. Patient 1 had had two invasive infections: a pneumococcal pneumonia with empyema (no previous pneumococcal vaccination) at the age of 9 years and a nosocomial *Staphylococcus aureus* osteomyelitis after surgical osteosynthesis at the age of 10 years; Patient 2 had had two episodes of otitis media (at 4 and 5 years of age), the first one with effusion, and had had one urinary tract infection (>10^5 colony-forming units of *Escherichia coli* per milliliter) at the age of 6 years. No other severe or recurrent infections were reported, and no long-term anti-infectious therapies were reported. The patients had no complications after routine vaccinations, including live viral vaccines. Patient 1 has attended a special education program since

kindergarten and has therefore presumably been exposed to infectious diseases; Patient 2 is home-schooled owing to a more severe neurologic phenotype.

Both patients were evaluated through the National Institutes of Health (NIH) Undiagnosed Disease Program and the NIH Primary Immune Deficiency Clinic. On the basis of the biochemical and genetic findings, the siblings were given a diagnosis of CDG-IIb (Fig. 1A, and Section S1 in the Supplementary Appendix, available with the full text of this article at NEJM.org).

STUDIES OF CDG-II$_B$ AND IMMUNOGLOBULIN

MOGS expression was assessed by means of immunoblotting of lysates from B cells that had been transformed by Epstein–Barr virus (EBV). The plasma IgG N-glycan profile was evaluated by means of MALDI-TOF (matrix-assisted laser detection desorption ionization–time-of-flight) mass spectrometry.[3] Unfolded-protein response and endoplasmic reticulum–associated degradation were tested in EBV-transformed B-cell lines. In vitro immunoglobulin production was evaluated with the use of an enzyme-linked immunosorbent spot (ELISPOT) assay,[4] and immunoglobulin half-life was studied by measuring human immunoglobulin in recombinant-activating gene 1 (Rag1)–knockout mice that were injected subcutaneously with human plasma (Section S2 in the Supplementary Appendix).

ASSAYS FOR VIRAL INFECTIONS

Cells from the siblings and healthy donors were tested for susceptibility to various viral infections. Human immunodeficiency virus (HIV) entry was explored with the use of four strains of HIV (BAL, IIIB, ELI6,[5] and BR) on CD8-depleted, CD4+ T cells[6] and evaluated by means of a realtime polymerase-chain-reaction (PCR) assay. For viral replication, HIV p24 protein levels were determined by means of an enzyme-linked immunosorbent assay (ELISA)[7]; for secondary infection, p24-normalized ELI6 virus recovered from the cells of the two patients and a healthy donor was evaluated in a viral-entry assay. The N-glycosylation pattern of the HIV envelope glycoprotein 140 was evaluated on transfected fibroblast cell lines,[4] and viral preparations recovered from transfected fibroblasts obtained from the patients were evaluated on TZM-bl indicator cells (genetically engineered HeLa cells that express CD4, CXCR4, and CCR5).

Influenza A virus entry and replication were evaluated on monocyte-derived macrophages with the use of the virus that caused the 2009 influenza A (H1N1) pandemic.[8] The viral load was measured according to hemagglutination and the 50% tissue-culture infective dose (TCID$_{50}$),[9] which is the quantity of virus required for a cytopathic effect in 50% of inoculated cultures; secondary infection was evaluated on Madin–Darby canine kidney (MDCK) cells.

Adenovirus type 5 entry, replication, and secondary infection were evaluated on primary fibroblasts according to the cytopathic effect and the results of a quantitative PCR assay.[10] Poliovirus 1 (PV1) entry, replication, and secondary infection were evaluated on primary fibroblasts and HeLa cells with the use of the Mahoney PV1 strain, according to the end point of titration, TCID$_{50}$, and cytopathic effect. Vaccinia virus entry, replication, and

secondary infection were evaluated on EBV-transformed B cells that had been infected with a recombinant vaccinia virus that expresses green fluorescent protein (Section S3 in the Supplementary Appendix).

RESULTS

BIOLOGIC ACTIVITY OF CDG-II$_B$ AND IMMUNOGLOBULIN

The levels of three abnormal N-linked high-mannose glycans (consisting of the following molecules: 3 glucose, 7 mannose, and 2 *N*-acetylglucosamine; 3 glucose, 8 mannose, and 2 *N*-acetylglucosamine; and 3 glucose, 9 mannose, and 2 *N*-acetylglucosamine) were significantly elevated in the purified plasma IgG from the patients, and the presence of N-linked glycans consisting of 3 glucose, 7 mannose, and 2 *N*-acetylglucosamine molecules at a mass-to-charge ratio of 2600.1 was unique to CDG-IIb (Fig. 1B). Moreover, the number of normal N-linked glycans, particularly high-mannose glycans (e.g., glycans consisting of 6 mannose and 2 *N*-acetylglucosamine molecules), was reduced. This pattern of changes in protein glycosylation was also observed in the N-glycan profile for total glycoproteins of fibroblasts cultured from the skin of the patients. In addition to IgG, other plasma proteins also had abnormal N-glycosylation patterns (section S4 in the Supplementary Appendix).

The two siblings had normal or increased numbers of B cells in the peripheral blood, and examination of a bone marrow aspirate and biopsy specimen from Patient 1 showed normal numbers of plasma cells. No evidence of protein loss through the gastrointestinal or genitourinary tract was identified, since α_1-antitrypsin clearance and a 24-hour urine specimen, respectively, were normal. Antibody levels to recall antigens were evaluated before and after the administration of booster doses of diphtheria–tetanus–acellular pertussis, conjugated *Haemophilus influenzae* type B, and hepatitis B vaccines, as well as 23-valent pneumococcal polysaccharide vaccine. Despite severe hypogammaglobulinemia, adequate immune responses to the four challenge vaccines developed. However, the results of tests for antibodies to measles, mumps, rubella, and varicella were negative or equivocal, despite adequate vaccination for age (each child had received two doses of the combined measles–mumps–rubella [MMR] and varicella vaccines, at approximately 1 and 5 years of age) (Table 1).

Two systems (unfolded-protein response and endoplasmic reticulum–associated degradation) that are responsible for the quality control of protein synthesis and for the degradation of misfolded N-glycosylated proteins[1] were within the normal limits of activity, and the two systems responded similarly to controls when stimulated with tunicamycin (an inducer of unfolded-protein response) or MG-132 (an inducer of endoplasmic reticulum–associated degradation) (Fig. 1C).

No reduction in the frequencies of antibody-secreting cells that were generated in vitro was detected, with the exception of IgA antibody–secreting cells in Patient 1. In addition, the amount of immunoglobulin secreted into the culture supernatants was similar for the patients and the healthy control, and the IgG from the patients did not undergo accelerated degradation after incubation at room temperature or at 4°C (Fig. 1D).

As shown in Figure 1E, plasma IgG from patients with CDG-IIb cleared significantly more rapidly (half-life, 6 days) than did plasma IgG from healthy controls (half-life, 21 days) when injected into Rag1$^{-/-}$ mice. Surface-plasmon-resonance experiments showed that purified IgG from the patients with CDG-IIb and the healthy control had similar binding affinities to immobilized FcγRIa and FcγRIIIb receptors and the neonatal Fc receptor (FcRn), a receptor known to contribute to the half-life of immunoglobulins (Section S5 in the Supplementary Appendix). IgG derived from the patients bound FcγRIIa with significantly lower affinity than did IgG from healthy controls.

CDG-II$_B$ AND SUSCEPTIBILITY TO VIRAL INFECTIONS

Viral entry into the cells of the two siblings with CDG-IIb and into the cells of unaffected controls was similar for the four strains of HIV tested (Fig. 2A). However, productive HIV replication, as measured by the amount of virus released into the culture supernatant, was 3.6 to 89.0 times as high in control cells as in the patients' cells. No differences were observed among HIV strains that use CCR5 or CXCR4. The possibility that the patients' serum, purified IgG, or other secreted factors could be contributing to the reduced HIV replication (Fig. 2A) was considered but ruled out (section S6 in the Supplementary Appendix). When we compared the infectivity of p24-normalized ELI6 virus produced in cells from the patients with CDG-IIb with that in cells from healthy controls, the virus that we recovered from the cells of the patients with CDG-IIb was 50 to 80% less infectious. Furthermore, binding of the glycandependent anti–HIV envelope antibody 2G12 to virus produced by cells from patients with CDG-IIb was reduced as compared with binding to virus produced by control cells, although no differences in binding were detected with the glycan-independent anti–HIV envelope antibody b12 (Section S7 in the Supplementary Appendix).

These differences in protein glycosylation were confirmed by the expression of HIV glycoprotein 140 in fibroblasts from the patients and healthy controls (Fig. 2B). The glycosylation pattern detected in cells from the healthy controls was induced into cells from the patients by transfection with a nonmutant MOGS expression vector, and conversely, the glycosylation pattern detected in cells from the patients was generated in control cells after treatment with the MOGS inhibitor castanospermine. Finally, the infectivity of HIV produced in fibroblasts from the patients was significantly enhanced when normal glycosylation was provided by cotransfection with the nonmutant MOGS expression vector (Fig. 2B).

Three different macrophage cultures were generated for each patient and infected with the virus that caused the 2009 influenza A (H1N1) pandemic. This resulted in one productive infection from one patient (Patient 1), whereas all three cultures from the control were efficiently infected. The virus collected from the culture from Patient 1 had lower hemagglutination titers and TCID$_{50}$ than did virus collected from the cultures from the healthy control. When equivalent amounts of virus collected from the macrophage cultures were used to infect influenzasusceptible MDCK cells, only one of three MDCK cell cultures infected with virus generated by macrophages from Patient 1 had evidence of a cytopathic effect and a positive result of a hemagglutination assay. In contrast, all three MDCK cell

cultures infected with virus from the control macrophages developed obvious signs of infection, with a marked cytopathic effect and highly positive hemagglutination titers (Fig. 2C, and Section S8 in the Supplementary Appendix).

A similar evaluation strategy was used to test primary infection, viral replication, and infectivity of virus recovered from cells infected with adenovirus type 5, PV1, and vaccinia virus. Adenovirus and PV1 infections of primary fibroblasts derived from patients and controls showed consistent results. Vaccinia virus infection of EBV-transformed B-cell lines from patients and controls also showed no marked differences in terms of sensitivity to infection, viral replication, or infectivity of progeny virus (Fig. 2D, 2E, and 2F).

DISCUSSION

In most cases, primary immunodeficiencies lead to an increased susceptibility to particular infectious diseases, but in the two siblings with severe hypogammaglobulinemia and CDG-IIb whom we evaluated, the outcome was different. Despite hypogammaglobulinemia, neither patient had recurrent sinopulmonary or severe viral infections. In contrast, immunocompetent children frequently present with 3 to 10 upper respiratory infections plus 1 to 4 cases of otitis media per year during infancy, most of which are caused by viruses.[11,12] The incidence and severity of infections are markedly increased in patients with severe hypogammaglobulinemia as a primary immunodeficiency.[13] The apparent paradox of severe hypogammaglobulinemia without a corresponding increase in infectious events prompted further investigation of the immune systems of the two siblings in this case.

Several causative mechanisms and pathways for hypogammaglobulinemia in the two patients were explored and eliminated: no protein loss was detected; B cells and plasma cells were normal in vivo; normal unfolded-protein response and endoplasmic reticulum–associated degradation activity in B cells argued against increased degradation of abnormally N-glycosylated immunoglobulins; and the in vitro evaluation of IgG synthesis, secretion, and stability did not reveal any abnormalities. However, in vivo analyses of serum IgG in Rag1$^{-/-}$ mice infused with plasma from the patients or the unaffected controls showed that the half-life of IgG in the patients was significantly reduced as compared with that of the healthy controls. Intrinsic defects in immunoglobulins due to N-glycosylation disorders represent a new explanation for hypogammaglobulinemia. However, the mechanism underlying the shortened IgG half-life in patients with CDG-IIb remains uncertain, although surface-plasmon-resonance analysis suggests that altered binding to FcγRIa, FcγRIIIb, and FcRn is unlikely to be involved. Whether the lower FcγRIIa binding affinity that has been observed in IgG from patients with CDG-IIb, as compared with healthy controls, contributes to their shortened half-life remains to be investigated.

Along with the severe hypogammaglobulinemia, we observed a peculiar antibody response pattern in the patients with CDG-IIb. The siblings had normal antibody responses to proteins, polysaccharides, and conjugated protein–polysaccharide immunogens that originated from nonreplicating infectious agents, but not to live viral vaccines such as MMR or varicella, which are viruses with glycosylated envelopes. Active viral replication is a necessary step to elicit protective antibody responses from these enveloped viruses, which

also depend on viral glycoproteins synthesized by infected host cells for viral egress, as well as viral entry into new susceptible cells.[14,15] In addition, several human viral receptors are themselves glycosylated proteins, which suggests that viral entry may also depend on host protein glycosylation.[14] In light of the dichotomous responses to vaccines consisting of live viruses and those not consisting of live viruses, we considered the possibility that N-glycosylation defects in patients with CDG-IIb were responsible for reduced susceptibility to infection with enveloped viruses that depend on glycosylation for productive infection.[14] Our results show that these patients do not have an altered susceptibility to adenovirus or PV1, which are nonenveloped viruses, or to vaccinia virus, which is an enveloped virus that does not depend on glycosylation for entry or egress.[16] In contrast, the patients do have a markedly reduced susceptibility to infection with HIV and influenza viruses, which are glycosylationdependent enveloped viruses. Although we cannot make broad generalizations, these data appear to suggest that altered glycosylation might modify the susceptibility to infection with viruses that must undergo protein glycosylation to complete their infection cycle.

Furthermore, as suggested by the effects of castanospermine on viral glycoproteins (Fig. 2B), there is a strong potential benefit of using inhibitors of MOGS as a means of controlling viral infections, especially those that pose a threat of rapid global spreading. Previous in vitro studies have shown that MOGS inhibitors such as castanospermine, *N*-butyldeoxynojirimycin (miglustat; previously known as NB-DNJ), or deoxynojirimycin can reduce viral replication in HIV infection, dengue, herpes simplex virus type 2 infection, and hepatitis C.[17-20] In a clinical study, patients with HIV-1 infection who received a combination of NB-DNJ and zidovudine had lower plasma viremia and higher CD4+ T-cell counts throughout the study than did patients who received zidovudine alone.[21] The side effects of combination therapy were not severe and included flatulence, diarrhea, paresthesias, and mild decreases in the hemoglobin level and platelet and neutrophil counts, as compared with treatment with zidovudine alone.

The reason for the absence of frequent, severe bacterial infections in these two patients with hypogammaglobulinemia remains unclear. The preserved rates of immunoglobulin production and functional antibody responses to bacterial antigens that we observed, together with normal complement levels and activity, normal respiratory burst, and normal cytokine production in response to bacterial agonists, phagocytosis, and lysis (data not shown), may contribute to the relatively benign infectious history of the siblings.[22] However, it is difficult to quantify the exposure to pathogens over time, since one child was homeschooled.

In summary, the two siblings we describe have a paradoxical clinical phenotype of severe hypogammaglobulinemia and increased resistance to particular viral infections. We evaluated the patients' immune systems and susceptibility to viral diseases and found an association with a rare MOGS N-glycosylation defect.

Supplementary Material

Refer to Web version on PubMed Central for supplementary material.

Acknowledgments

References

1. Varki, A. Essentials of glycobiology. 2nd ed.. Cold Spring Harbor Laboratory Press; Cold Spring Harbor, NY: 2009.

2. De Praeter CM, Gerwig GJ, Bause E, et al. A novel disorder caused by defective biosynthesis of N-linked oligosaccharides due to glucosidase I deficiency. Am J Hum Genet. 2000; 66:1744–56. [PubMed: 10788335]

3. Faid V, Chirat F, Seta N, Foulquier F, Morelle W. A rapid mass spectrometric strategy for the characterization of N- and O-glycan chains in the diagnosis of defects in glycan biosynthesis. Proteomics. 2007; 7:1800–13. [PubMed: 17520685]

4. Buckner CM, Moir S, Ho J, et al. Characterization of plasmablasts in the blood of HIV-infected viremic individuals: evidence for nonspecific immune activation. J Virol. 2013; 87:5800–11. [PubMed: 23487459]

5. Moir S, Lapointe R, Malaspina A, et al. CD40-mediated induction of CD4 and CXCR4 on B lymphocytes correlates with restricted susceptibility to human immunodeficiency virus type 1 infection: potential role of B lymphocytes as a viral reservoir. J Virol. 1999; 73:7972–80. [PubMed: 10482544]

6. Chun TW, Justement JS, Murray D, et al. Rebound of plasma viremia following cessation of antiretroviral therapy despite profoundly low levels of HIV reservoir: implications for eradication. AIDS. 2010; 24:2803–8. [PubMed: 20962613]

7. Chun TW, Nickle DC, Justement JS, et al. Persistence of HIV in gut-associated lymphoid tissue despite long-term antiretroviral therapy. J Infect Dis. 2008; 197:714–20. [PubMed: 18260759]

8. Gorry PR, Bristol G, Zack JA, et al. Macrophage tropism of human immunodeficiency virus type 1 isolates from brain and lymphoid tissues predicts neurotropism independent of coreceptor specificity. J Virol. 2001; 75:10073–89. [PubMed: 11581376]

9. Szretter KJ, Balish AL, Katz JM. Influenza: propagation, quantification, and storage. Curr Protoc Microbiol. 2006; 15:15G1.

10. Di Pasquale G, Chiorini JA. PKA/PrKX activity is a modulator of AAV/adenovirus interaction. EMBO J. 2003; 22:1716–24. [PubMed: 12660177]

11. Henderson FW, Collier AM, Sanyal MA, et al. A longitudinal study of respiratory viruses and bacteria in the etiology of acute otitis media with effusion. N Engl J Med. 1982; 306:1377–83. [PubMed: 6281639]

12. Chonmaitree T, Revai K, Grady JJ, et al. Viral upper respiratory tract infection and otitis media complication in young children. Clin Infect Dis. 2008; 46:815–23. [PubMed: 18279042]

13. Winkelstein JA, Marino MC, Lederman HM, et al. X-linked agammaglobulinemia: report on a United States registry of 201 patients. Medicine (Baltimore). 2006; 85:193–202. [PubMed: 16862044]

14. Fields, BN.; Knipe, DM.; Howley, PM. Fields virology. 5th ed.. Wolters Kluwer Health/Lippincott Williams & Wilkins; Philadelphia: 2007.

15. Obaro SK, Pugatch D, Luzuriaga K. Immunogenicity and efficacy of childhood vaccines in HIV-1-infected children. Lancet Infect Dis. 2004; 4:510–8. [PubMed: 15288824]

16. Moss B. Poxvirus entry and membrane fusion. Virology. 2006; 344:48–54. [PubMed: 16364735]

17. Ahmed SP, Nash RJ, Bridges CG, et al. Antiviral activity and metabolism of the castanospermine derivative MDL 28,574, in cells infected with herpes simplex virus type 2. Biochem Biophys Res Commun. 1995; 208:267–73. [PubMed: 7887939]

18. Schul W, Liu W, Xu HY, Flamand M, Vasudevan SG. A dengue fever viremia model in mice shows reduction in viral replication and suppression of the inflammatory response after treatment with antiviral drugs. J Infect Dis. 2007; 195:665–74. [PubMed: 17262707]

19. Fischer PB, Karlsson GB, Dwek RA, Platt FM. N-butyldeoxynojirimycin-mediated inhibition of human immunodeficiency virus entry correlates with impaired gp120 shedding and gp41 exposure. J Virol. 1996; 70:7153–60. [PubMed: 8794362]

20. Qu X, Pan X, Weidner J, et al. Inhibitors of endoplasmic reticulum alphaglucosidases potently suppress hepatitis C virus virion assembly and release. Antimicrob Agents Chemother. 2011; 55:1036–44. [PubMed: 21173177]

21. Fischl MA, Resnick L, Coombs R, et al. The safety and efficacy of combination N-butyl-deoxynojirimycin (SC-48334) and zidovudine in patients with HIV-1 infection and 200-500 CD4 cells/mm^3. J Acquir Immune Defic Syndr. 1994; 7:139–47. [PubMed: 7905523]

22. Stiehm ER. Human intravenous immunoglobulin in primary and secondary antibody deficiencies. Pediatr Infect Dis J. 1997; 16:696–707. [PubMed: 9239774]

A MOGS Expression

B N-Glycan Profile of IgG

C Unfolded-Protein Response and Endoplasmic Reticulum–Associated Degradation

D In Vitro Immunoglobulin Production and Secretion

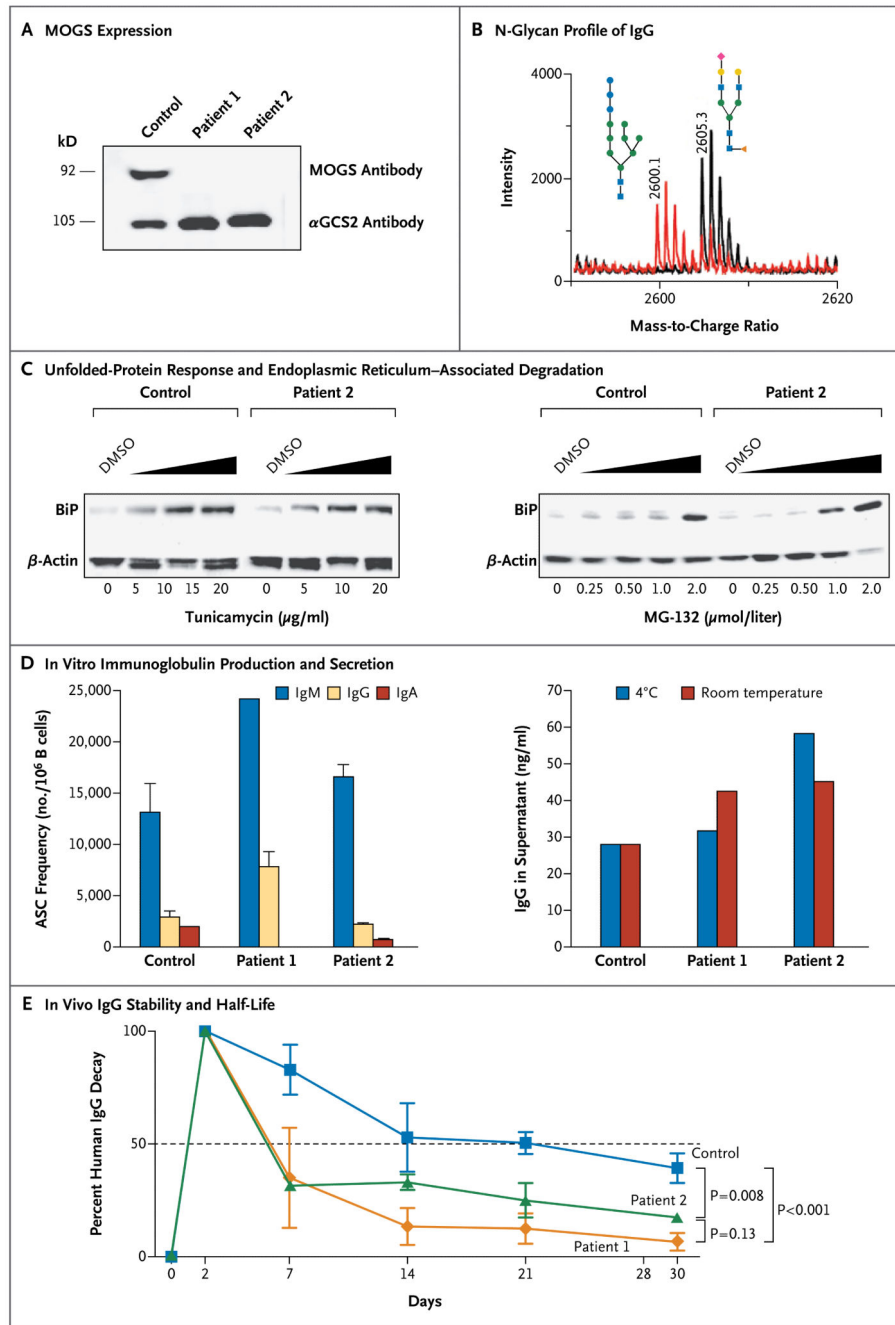**E** In Vivo IgG Stability and Half-Life

Figure 1. Mannosyl-Oligosaccharide Glucosidase (MOGS) Expression and Immunoglobulin Studies in Two Siblings with Congenital Disorder of Glycosylation Type IIb (CDG-IIb)

The immunoblot in Panel A shows MOGS expression in the patients with CDG-IIb. Protein lysates were obtained from Epstein–Barr virus (EBV)–transformed B-cell lines from patients and controls and hybridized with antibodies against MOGS and alpha-glucosidase 2 (*a*GCS2); *a*GCS2 was readily detected on the B-cell lysates from a healthy control and from the patients, but MOGS was not detected on the B-cell lysates from the patients.

Panel B shows the N-glycan profile of purified IgG from Patient 2 with CDG-IIb (red) and a healthy control (black), assessed by means of MALDI-TOF (matrix-assisted laser detection

desorption ionization–time-of-flight) mass spectrometry. The patient had increased high-mannose glycans (consisting of 3 glucose, 7 mannose, and 2 *N*-acetylglucosamine molecules, shown at a mass-to-charge ratio of 2600.1) and decreased normal glycans (consisting of 1 *N*-acetylneuraminic acid, 4 *N*-acetylglucosamine, 3 mannose, and 1 fucose, shown at a mass-to-charge ratio of 2605.3). The blue squares denote *N*-acetylglucosamine, green circles mannose, blue circles glucose, yellow circles galactose, red rhombus *N*-acetylneuraminic acid, and orange triangle fucose.

The immunoblots in Panel C show the level of expression of binding immunoglobulin protein (BiP), a molecular chaperone in the endoplasmic reticulum that is up-regulated during endoplasmic reticulum stress, in the EBV-transformed B cells from a healthy control and from Patient 2, which were treated with increasing doses of tunicamycin (an inducer of unfolded-protein response through competitive inhibition of *N*-acetylglucosamine-1-phosphotransferase) and MG-132 (an inducer of endoplasmic reticulum-associated degradation through proteasome inhibition) for 16 hours. Dimethyl sulfoxide (DMSO) solvent was used in the reconstitution of tunicamycin and MG-132 and was added to cells in adjusted amounts as a negative control for stress. β-actin was used as a loading control. Representative results of multiple experiments are shown.

Panel D shows in vitro production and secretion of immunoglobulin, evaluated with the use of antibody-secreting cells (ASCs) differentiated from the B cells of Patient 1, Patient 2, and a healthy control. Peripheral-blood mononuclear cells were stimulated with *Staphylococcus aureus* Cowan (SAC) particles and CpG-containing oligonucleotides, and ASC frequencies were evaluated by means of an enzyme-linked immunospot assay. Except for IgA ASCs in Patient 1, ASC frequencies in the patients were similar to those in the healthy control (left graph). IgG produced by ASCs was collected and stored at −20°C. Samples were thawed and kept overnight at 4°C or room temperature before evaluation of IgG levels (right graph). T bars represent standard deviations. Representative results of multiple experiments are shown.

Panel E shows in vivo IgG stability and half-life in Rag1-knockout mice subcutaneously injected with plasma from the patients or healthy controls. The plasma had been normalized to contain equal amounts of IgG (1 mg or 2.5 mg). Levels of human IgG in the mice were sequentially monitored and analyzed with the use of a two-way analysis of variance with repeated measures and correction for multiple comparisons (Bonferroni's t-test). I bars represent standard errors. Representative results of multiple experiments are shown.
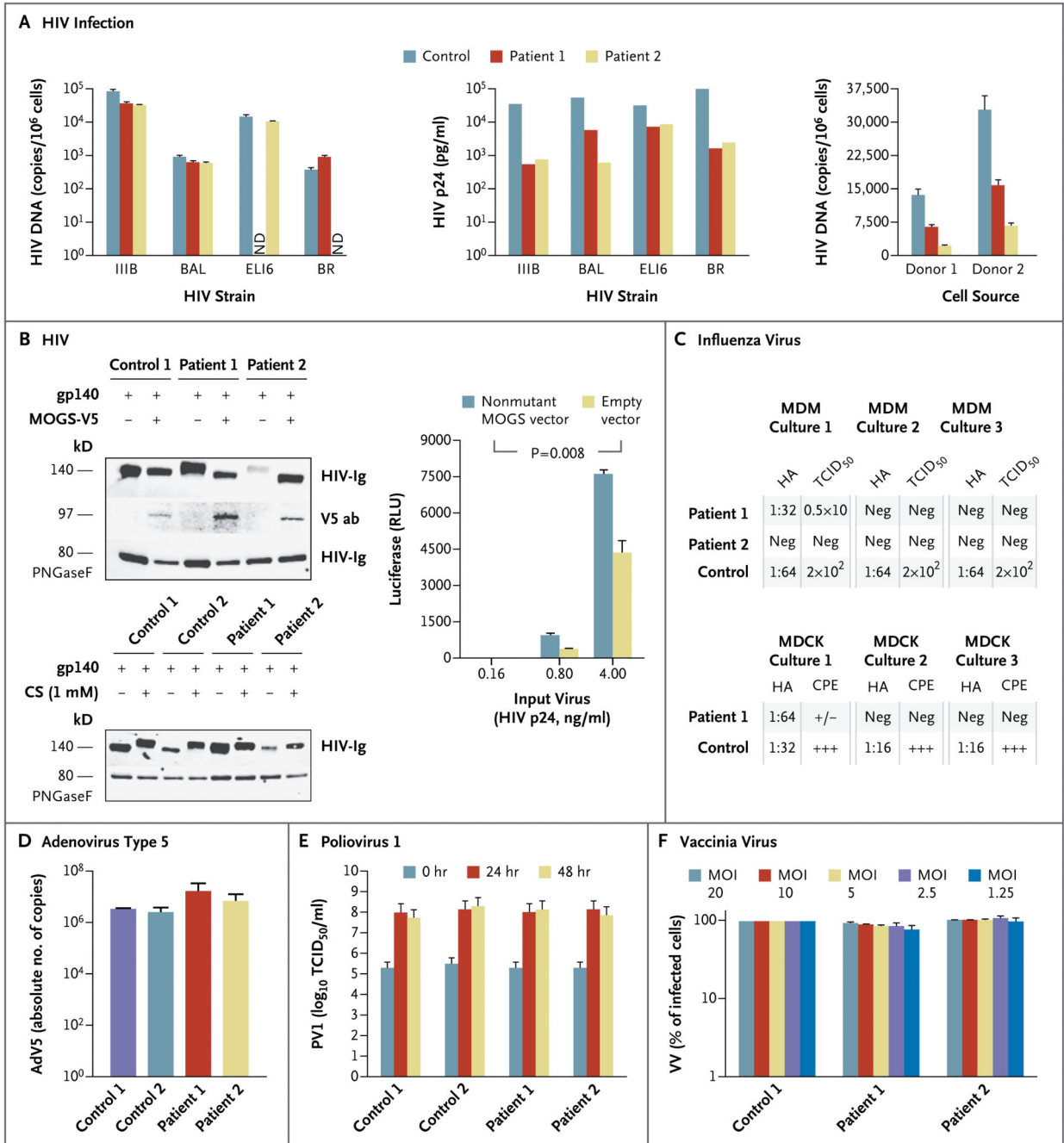
Figure 2. Viral Susceptibility Studies in the Patients

Panel A shows human immunodeficiency virus (HIV) infection experiments. The left graph shows entry of four HIV strains into activated, CD8-depleted peripheral-blood mononuclear cells (PBMCs) from a healthy control and from the two patients with CDG-IIb. Target cells were incubated with the various strains of HIV for 2 hours at 37°C. After extensive washing, the cells were lysed, and a real-time polymerase-chain-reaction (PCR) assay specific for HIV DNA was performed. T bars represent standard deviations. Data are representative of three independent experiments. ND denotes not done. The middle graph shows the level of

HIV replication under the same conditions as those used to assess viral entry. Infected cells were maintained at 37°C, culture supernatants were harvested, and the HIV p24 protein level was determined by means of enzyme-linked immunosorbent assay (ELISA). Data shown represent the level of viral replication at day 3 or day 4 after infection. Data are representative of four independent experiments. The right graph shows viral entry of the ELI6 strain, recovered at day 4 from each cell culture performed for the assessment of HIV p24. Target cells from two healthy donors were prepared by activating their PBMCs for 2 days, followed by purification of their CD4+ T cells. The amount of virus from each of the three sources that was incu bated with target cells was normalized according to the level of p24 measured by ELISA in the culture supernatant. A realtime PCR assay specific for HIV DNA was performed. T bars represent standard deviations.

In Panel B, the top immunoblot shows primary fibroblast lysates from the patients and controls, which were transfected with an HIV glycoprotein 140 (gp140)-coding vector with or without a V5-tagged nonmutant mannosyl-oligosaccharide glucosidase (MOGS)–expression vector. As expected on the basis of their N-glycan trimming defect, the viral gp140 synthesized in the cells from the patients had a higher molecular weight than that synthesized in the control cells. When the cells from the patients were transfected with the nonmutant MOGS-V5 vector, the gp140 molecular weight reverted to the control molecular weight. The differences in molecular weight depended on the N-glycosylation pattern, as revealed after N-glycan removal by means of peptide-N-glycosidase F (PNGaseF) digestion. The bottom immunoblot shows the same distinctive HIV gp140 glycosylation pattern detected in cells from the controls and those from the patients, but in this case, the gp140 glycosylation pattern detected in the control cells was induced into the patients' pattern by the MOGS inhibitor castanospermine (CS). HIV-Ig denotes rabbit polyclonal antihuman HIV antibody, and V5 ab mouse monoclonal anti-V5 antibody. The graph shows the infectivity of HIV produced in fibroblasts from Patient 2, which was greater after cotransfection of fibroblasts with nonmutant MOGS than with empty expression vector. RLU denotes relative light units. T bars represent standard deviations. The P value is based on a two-way analysis of variance with repeated measures. Data are representative of three independent experiments.

In Panel C, the upper chart shows viral titers after infection of cells from Patient 1, Patient 2, and a healthy control with the virus that caused the 2009 influenza A (H1N1) pandemic. Viral titers were assessed on the basis of hemagglutination (HA) and the 50% tissue-culture infective dose ($TCID_{50}$) of the virus produced by monocyte-derived macrophages (MDM) from the patients and the healthy control (three cultures per person). No virus was isolated from any of the MDM cultures from Patient 2. Only one of the cultures from Patient 1 replicated the virus, but the titer was 1.5 log lower than that in the control cells. The lower chart shows HA titers and evidence of a cytopathic effect (CPE) in Madin–Darby canine kidney (MDCK) cells that were infected with equivalent amounts of influenza virus produced by MDM cultures from Patient 1 and a control. Only one of three cultures incubated with virus from Patient 1 had a positive HA titer and minimal CPE (+/−). CPE and HA titers were negative (Neg) in the other two cultures. All three MDCK cultures that were infected with virus that was produced by the control cells showed marked CPE (+++) and positive HA titers.

Panel D shows the results of a secondary-infection experiment in which adenovirus type 5 (AdV5) produced from fibroblasts obtained from patients and controls during primaryinfection experiments was normalized to infect control fibroblasts. Cells were lysed, and virus was measured in triplicate by means of a quantitative PCR assay. T bars represent standard deviations.

Panel E shows the results of a secondary-infection experiment in which poliovirus 1 (PV1, Mahoney strain) produced from fibroblasts obtained from patients and controls during primary-infection experiments was normalized to infect HeLa cells. The CPE was assessed 72 hours after inoculation, and titers were calculated with the use of the Reed and Muench method. T bars represent standard errors.

Panel F shows the results of a secondary-infection experiment in which vaccinia virus (VV) produced from EBV-transformed B-cell lines obtained from the patients and a control during primary-infection experiments was normalized to infect control EBV-transformed B-cell lines. Cells were lysed, and serial dilutions of the cell lysates were tested for their ability to infect B cells from a healthy donor. MOI denotes multiplicity of infection. T bars represent standard deviations.

Table 1

Immunologic Characteristics of Two Siblings with Congenital Disorder of Glycosylation Type lib (CDG-IIb).[*]

Variable	Reference Range[†]	Patient 1	Patient 2
Plasma IgG — mg/dl	572–1474	317	142
Plasma IgA — mg/dl	34–305	<7	17
Plasma IgM — mg/dl	32–208	21	21
Plasma IgE — mg/dl	0–90	9.2	7.9
Anti-tetanus toxoid antibodies — IU/ml	>0.15		
Before vaccination		<0.16	0.18
After vaccination		>7	3.88
Anti–diphtheria toxoid antibodies — IU/ml	>0.1		
Before vaccination		0.11	0.13
After vaccination		>3	2.87
Anti–*Haemophilus influenzae* type B antibodies — mg/liter	>0.15		
Before vaccination		0.24	0.15
After vaccination		>9	>9
Anti-pneumococcal antibody titer 1.3 μg/dl — no./total no.[‡]			
Before vaccination		2/23	2/23
After vaccination		15/23	12/23
Anti–hepatitis B surface antigen antibodies — IU/ml	>10		
Before vaccination		Negative	Negative
After vaccination		>12	>12
Anti-measles IgG antibodies[§]		Negative	Equivocal
Anti-mumps IgG antibodies[§]		Equivocal	Negative
Anti-rubella IgG antibodies		Negative	Negative
Anti-varicella IgG antibodies		Negative	Negative
Anti-influenza antibodies, hemagglutination-inhibition assay	Negative		
Seasonal H1N1		Negative	Negative
H3N2		Negative	Negative
2009 influenza A, H1N1		Negative	Negative
Anti-B antibodies, isohemagglutinin titer	1:8	1:2	1:16
Albumin — g/dl	2.9–4.2	4.2	4.1
Plasma complement			
C3 — mg/dl	90–180	120	130
C4 — mg/dl	10–40	16	17
CH50 — CAE units[¶]	55–145	130	103

Sadat et al.

Variable	Reference Range[†]	Patient 1	Patient 2
White-cell count — per mm³	4500–11,000	14,880	12,700
Differential count — %			
Neutrophils	40–70	23	13
Lymphocytes	22–44	67	78
Monocytes	4–11	6	7
Eosinophils	0–8	2	2
Basophils	0–3	2	0
Dihydrorhodamine test		Normal	Normal
Lymphocyte proliferation assay, with phytohemagglutinin stimulation — counts/min	40,000–150,000	202,162	186,154
CD3+ lymphocytes — cells/mm³ (%)	1200–2600 (60–76)	7145 (71.7)	2469 (65)
CD4+ lymphocytes	650–2500 (31–47)	3844 (38.6)	1788 (47)
CD8+ lymphocytes	370–1100 (18–35)	2879 (28.9)	553 (14.6)
CD16+/CD56+ lymphocytes — cells/mm³ (%)	100–480 (4–17)	759 (7.6)	150 (4)
CD19+ lymphocytes — cells/mm³ (%)	270–860 (3–19)	2086 (20.9)	1220 (32.1)
CD19+ IgM		2025 (20.3)	1115 (29.3)
CD19+ IgD		2000 (20.1)	1124 (29.4)
CD19+ IgG		33 (0.3)	45 (1.2)
CD19+ IgA		2 (<0.1)	22 (0.6)
CD19+/CD27+		602 (6.1)	93 (2.4)

[*] Antibody titers were evaluated after completion of a regular vaccination program for measles, mumps, rubella, and varicella or 1 month after vaccination with diphtheria–tetanus–acellular pertussis, *Haemophilus influenzae* B, 23-valent pneumococcal polysaccharide, and recombinant hepatitis B (Section S9 in the Supplementary Appendix).

[†] The reference range for titers indicates protective titers.

[‡] Values are the number of serotypes with protective titers (i.e., 1.3 μg per deciliter) divided by the number of serotypes tested.

[§] "Equivocal" denotes equivocal results of two tests.

[¶] CAE denotes complement activity enzyme immunoassay units.